Intermetallics 45 (2014) 5–10

Contents lists available at ScienceDirect

Intermetallics

journal homepage: www.elsevier.com/locate/intermet

Drastic changes of electronic structure, bonding properties and crystal symmetry in Zr_2Cu by hydrogenation, from *ab initio*

Adel F. Al Alam [a], Samir F. Matar [b,c,*], Ahmad Jammal [d], Naïm Ouaini [a]

[a] Holy Spirit University of Kaslik, USEK, Jounieh, Lebanon
[b] CNRS, ICMCB, UPR 9048, F-33600 Pessac, France
[c] Univ. Bordeaux, ICMCB, UPR 9048, F-33600 Pessac, France
[d] Ministry of Higher Education, Beirut, Lebanon

ARTICLE INFO

Article history:
Received 22 July 2013
Received in revised form
13 September 2013
Accepted 16 September 2013
Available online 8 October 2013

Keywords:
A. Intermetallics, miscellaneous
B. Bonding
C. Interstitial content, control
E. Electronic structure, calculation

ABSTRACT

Gradual hydrogen uptake into Zr_2Cu intermetallic leads to crystal symmetry changes from tetragonal Zr_2CuH_2 to monoclinic Zr_2CuH_5. This experimental finding is explained here from cohesive energies computed within quantum DFT for Zr_2CuH_x ($x = 1, 2, 3, 4, 5$) models in both structures. The threshold is found at $2 < x < 3$ in agreement with experiment. Beside structural crossover, electronic properties, chemical bonding, and mechanical behavior are also analyzed. Metal–H interactions arising from increasingly H presence in Zr_2Cu lead to more and most cohesive and harder Zr_2CuH_2 and Zr_2CuH_5 respectively.

1. Introduction

Several binary intermetallic compounds based on zirconium are known as C15 *Laves* phases ZrT_2 [1] and Zr_2T [2], T being a transition metal. Besides mechanical properties in equiatomic ZrT such as the hardness sought for uses in biomedical materials [3] and shape memory applications [4], a major characteristic is in their ability of absorbing large amounts of hydrogen such as $ZrFe_2H_{3.5}$ [5], $ZrNiH_3$ [6] and Zr_2CuH_5 [7] which led to their investigation as potential candidates for hydrogen storage [8–10]. In this context, intermetallic Zr_2Cu belongs to the A_2Cu family (A = Ti, Zr, Hf) crystallizing in the body centered tetragonal $MoSi_2$-type (cf. Table 1) [8]. They can absorb hydrogen by occupying the [A_4] tetrahedral sites. The structure of Zr_2CuH_2 and tetrahedral H surroundings are shown in Fig. 1. Zr_2Cu hydrides can be of interest experimentally because they decompose slowly around 200 °C compared to 527 °C for similar Zr_2Pd [8]. This lets suggest significant iono-covalent character of hydrogen and lower enthalpies of formation.

The question arises as to whether more hydrogen can be absorbed while keeping the $MoSi_2$-type structure. In fact the hydrogen saturated compound Zr_2CuH_5 is found in a monoclinic structure shown in Fig. 1 with the different hydrogen environment [7]. The ordering of hydrogen often leads to structural distortion, e.g. body centered tetragonal Zr_2Co becomes primitive tetragonal with hydrogen ordering in Zr_2CoH_5 (cf. Ref. [11] and therein cited works). This is also observed in the cubic Laves phases C15 with Fm-3m space group (SG), which becomes monoclinic in $P1n1$ SG in saturated YFe_2H_5 [9].

It becomes subsequently relevant to examine the composition threshold at which the monoclinic phase stabilizes in Zr_2CuH_x based on energy criteria. These aspects and the effects of increasing amounts of hydrogen on the mechanical properties and the iono-covalent behavior of hydrogen can be addressed quantitatively in the framework of the quantum density functional theory (DFT) [12]. This is the aim of the present work.

2. Structural details

The structures of tetragonal Zr_2Cu and Zr_2CuH_2, and monoclinic Zr_2CuH_5 are described in Table 1 and sketched in Fig. 1. The di-hydrogenated ternary has the tetragonal $MoSi_2$-type structure ($I4/mmm$ space group SG). Fig. 1(a) shows H located in edge sharing [Zr_4] tetrahedra at (4d) Wyckoff position [7]. The saturated monoclinic structure has five coordination polyhedra for H as shown in Fig. 1(b): (i) tetrahedral [Zr_4] and [Zr_3Cu] coordinations, and (ii)

* Corresponding author. CNRS, ICMCB, UPR 9048, F-33600 Pessac, France. Tel.: +33 540002690; fax: +33 54002761.
E-mail addresses: matar@icmcb-bordeaux.cnrs.fr, abouliess@gmail.com (S.F. Matar).

0966-9795/$ – see front matter © 2013 Elsevier Ltd. All rights reserved.
http://dx.doi.org/10.1016/j.intermet.2013.09.009

Table 1
Experimental and (calculated) crystal data for Zr_2Cu, Zr_2CuH_2 and Zr_2CuH_5 [7,8]. SG: space group. FU = formula unit.

Zr_2Cu
SG#139 *I*4/*mmm*
$MoSi_2$, C11*b*-type
a = 3.120 (3.21) Å
c = 11.183 (11.23) Å
V = 108.86 (115.7101) Å^3

At.(Wyck.)	x	y	z
Cu (2*a*)	0	0	0
Zr (4*e*)	0	0	0.340 (0.345)

Total energy (eV)/FU: −21.08 eV

Zr_2CuH_2
SG#139 *I*4/*mmm*
$MoSi_2$, C11*b*-type
a = (3.256) Å
c = (11.796) Å
V = (125.06) Å^3
Hypo. 1

At. (Wyck.)	x	y	z
Cu (2*a*)	0	0	0
Zr (4*e*)	0	0	(0.361)
H (4*d*)	0	½	¼

d(Zr–H) = 2.09 Å
Total energy (eV)/FU: −29.13 eV

Hypo. 2: H (4*e*) 0 0 z ($z_{calc.}$ ~ 0.17): d(Zr–H) = 2.20 Å; $E_{TOT.}$ = −28.87 eV.
Hypo. 3: H (4*c*) 0 ½ 0 : d(Cu–H) = 1.73 Å; $E_{TOT.}$ = −28.04 eV.

Zr_2CuH_5
SG#12 *I*2/*m*
Exp. Ref. [7]
a = 9.336 (9.882) Å
b = 3.603 (3.667) Å
c = 8.343 (8.390) Å
β = 104.29° (103.93°)
V = 271.94 (278.06) Å^3.

At.(Wyck.)	x	y	z
Cu (4*i*)	0.3792 (0.377)	0	0.5250 (0.529)
Zr1 (4*i*)	0.0768 (0.081)	0	0.2320 (0.236)
Zr2 (4*i*)	0.6653 (0.683)	0	0.086 (0.100)
H1 (4*i*) (Zr_4)	0.1385 (0.134)	0	0.7211 (0.711)
H2 (4*i*) (Zr_4)	0.4617 (0.464)	0	0.1419 (0.140)
H3 (4*i*) (Zr_3Cu)	0.3155 (0.316)	0	0.2938 (0.296)
H4 (4*i*) (Zr_3Cu)	0.1883 (0.183)	0	0.4039 (0.482)
H5[a] (4*i*) (Zr_3Cu_2)	0.8895 (0.882)	0	0.0291 (0.022)

Shortest distances with H:
- Zr substructure: d(Zr–H1) = 2.07 Å; d(Zr–H2) = 2.06 Å; d(Zr–H3) = 2.13 Å; d(Zr–H4) = 2.02 Å; d(Zr–H5) = 2.20 Å.
- Cu substructure: d(Cu–H3) = 1.86 Å; d(Cu–H4) = 1.75 Å; d(Cu–H5) = 1.84 Å.

Total energy (eV)/FU: −40.46 eV.

[a] Experimental occupancy 0.71.

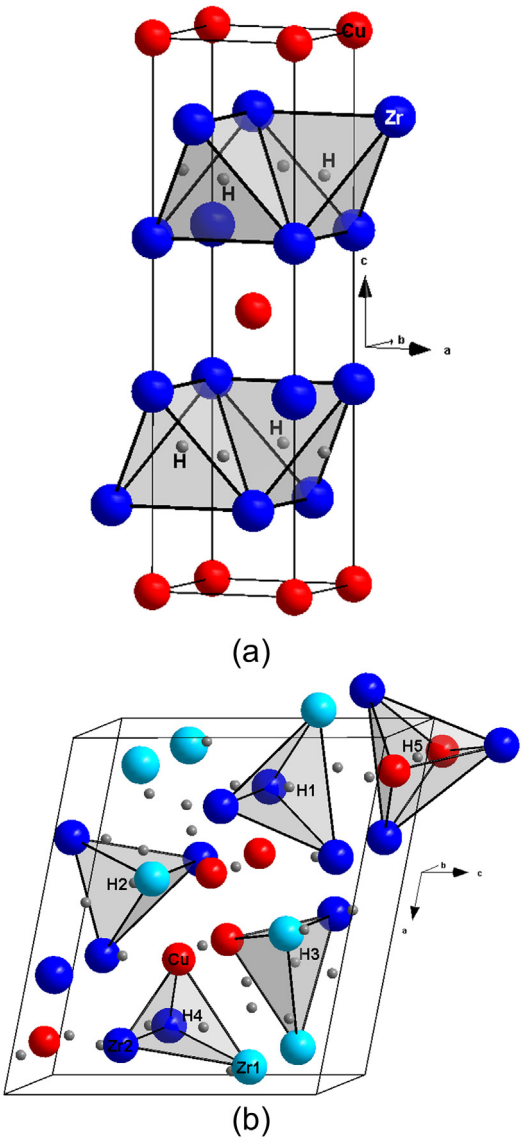

Fig. 1. Sketches of the crystal structure of: (a) tetragonal Zr_2CuH_2 with H in [Zr_4] tetrahedral site, and (b) the hydrogen rich monoclinic Zr_2CuH_5 showing the different environments of hydrogen atoms as given in Table 1.

prismatic [Zr_3Cu_2] coordination. The latter sites are partially populated by H. It is important to mention the similarity of the [Zr_4] coordination of H in both tetragonal and monoclinic structures, which lets suggest that the departure from such coordination in tetragonal structure should lead to destabilizing the ternary system. This is addressed in the upcoming sections.

Note that the determination of hydrogen positions from powder neuron diffraction data in the title compounds and in other compounds such as the intermediate hydrides of $MgPd_3$ [13] can be verified and predicted from computations as in the investigation of hydrogenated $LaNi_5$ and $LaCo_5$ [14].

3. Computation methods

Two computational methods within the DFT were used in a complementary manner. The Vienna ab initio simulation package (VASP) code [15] allows geometry optimization and total energy calculations. For this we use the projector augmented wave (PAW) method [16], built within the generalized gradient approximation (GGA) scheme following Perdew, Burke and Ernzerhof (PBE) [17]. Also preliminary calculations with local density approximation LDA [18] led expectedly to an underestimated volume versus the experiment. The conjugate-gradient algorithm [19] is used in this computational scheme to relax the atoms. The tetrahedron method with Blöchl corrections [16] as well as a Methfessel–Paxton [20] scheme were applied for both geometry relaxation and total energy calculations. Brillouin-zone (BZ) integrals were approximated using the special k-point sampling. The optimization of the structural parameters was performed until the forces on the atoms were less than 0.02 eV/Å and all stress components less than 0.003 eV/Å^3. The calculations are converged at an energy cut-off of 300 eV for the plane-wave basis set with respect to the k-point integration with a starting mesh of 4 × 4 × 4 up to 8 × 8 × 8 for best convergence and relaxation to zero strains. Using larger energy cut-off values as 500 eV did not lead to better convergence or to